

# Selectively $^{13}\text{C}$ -Enriched DNA: Dynamics of the $\text{C1'H1'}$ and $\text{C5'H5'}$ or $\text{C5'H5''}$ Vectors in $\text{d}(\text{CGCAAATTTGCG})_2$

Florence Gaudin, Luc Chanteloup, N. T. Thuong and G. Lancelot\*

Centre de Biophysique Moléculaire, CNRS, Rue Charles Sadron, F-45071 Orléans Cédex 2, France

In order to examine the internal dynamic processes of the dodecamer  $\text{d}(\text{CGCAAATTTGCG})_2$ , the  $^{13}\text{C}$ -enriched oligonucleotide was synthesized. The C3, A4 and A6 residues were selectively  $^{13}\text{C}$  labeled at the C1' and C5' positions and their  $R(\text{C}_{\alpha, \gamma})$ ,  $R(\text{C}_\alpha)$  and  $R(\text{H}_\alpha \rightarrow \text{C}_\alpha)$  relaxation rates were measured. Data variations were observed for the three residues. The analysis of the relaxation rates in the context of the model-free formalism of Lipari and Szabo indicates other pathways than those described by  $\tau_g$ ,  $S^2$  and  $\tau_i$ . Direct evidence for the presence of a conformational exchange process was obtained for the residue A4 from rotating frame relaxation measurements. Taking into account the exchange process contribution, analysis of these data gave a  $\tau_g$  value of 3.7 ns at 32 °C, in agreement with those computed from independent  $^{13}\text{C}$  relaxation rate measurements on the three thymines or from the H5–H6 NOE measurements. The frequency difference between the exchanging sites was computed in the range 130–250 Hz. This additional relaxation process involves large amplitude and slow motions ( $\tau_{\text{ex}} = 130 \mu\text{s}$ ) which can reflect special dynamics of the tract AAATTT which supports the spine of hydration. Analysis of  $^{13}\text{C}$  relaxation rates indicated smaller order parameters  $S^2$  for C5' (0.40) than for C1' (0.80). These data reflected additional motions undergone by the  $\text{C5'H5'}$  or  $\text{C5'H5''}$  vectors such as repuckering and motions around the C4'–C5' bond. © 1997 by John Wiley & Sons, Ltd.

*Magn. Reson. Chem.* 35, 561–565 (1997) No. of Figures: 3 No. of Tables: 2 No. of References: 2

**Keywords:** DNA; dynamics;  $^{13}\text{C}$  NMR; A tract

Received 10 June 1996; revised 11 September 1996; accepted 11 September 1996

## INTRODUCTION

NMR relaxation experiments can, as a rule, provide a detailed description of nucleic acid dynamics. Precise conclusions are, however, difficult to deduce from  $^1\text{H}$  spin relaxation rate measurements because several motions implicating a change in orientation and distances of the H–H vectors must be simultaneously taken into account to reflect the experimental data.  $^{13}\text{C}$  spin–lattice relaxation whose processes are governed by the changes in orientation of the  $^{13}\text{C}$ – $^1\text{H}$  vector, the length of which is constant, is easier to interpret. Therefore,  $^{13}\text{C}$  (or  $^{15}\text{N}$ ) NMR relaxation studies are the best choice for investigating the dynamic processes. This can be accomplished by measuring the six spin–lattice relaxation rates  $R(\text{C}_\alpha)$ ,  $R(\text{C}_{\alpha, \gamma})$ ,  $R(\text{H}_\alpha \rightarrow \text{C}_\alpha)$ ,  $R(2\text{H}_\alpha\text{C}_\alpha)$ ,  $R(2\text{H}_\alpha\text{C}_{\alpha, \gamma})$  and  $R(\text{H}_\alpha^\circ)$ , which allows one to compute the spectral density functions for five different frequencies.<sup>1</sup> Nevertheless, the calculated  $J(\omega)$  values are altered by accumulation of the uncertainties on each relaxation rate measurement. Consequently, more accurate information on both amplitude and rate of the internal motions will be extracted from the relaxation rates  $R(\text{C}_\alpha)$ ,  $R(\text{C}_{\alpha, \gamma})$  and  $R(\text{H}_\alpha \rightarrow \text{C}_\alpha)$ .<sup>2</sup>

In a previous paper,<sup>2</sup> we presented an approach to the internal dynamic processes of the three central

thymines in the selectively  $^{13}\text{C}$ -enriched dodecamer  $\text{d}(\text{CGCAAATTTGCG})_2$ . Experimental spin–lattice relaxation rates were simulated well by computing the effect of local and internal motions of the vector C1'–H1' on the density functions. Two models for the internal mobility of the base pairs and of sugars were presented for the three thymines. This dodecamer contains an  $\text{A}_3\text{T}_3$  tract which is known to induce special conformational properties. Inphase ligated  $\text{A}_n\text{T}_n$  segments experience retarded electrophoretic migration which has been widely interpreted as a result from macroscopic DNA curvature<sup>3,4</sup> and the ApT step was distinguished by slow base pair opening kinetics.<sup>5</sup> Moreover, Brown *et al.*<sup>6</sup> reported significantly different mobilities for the adenine and thymine residues in the crystal structure of  $\text{d}(\text{CGCAAATTTGCG})_2$ .

In order to compare first the dynamic processes of the C1' and C5' atoms and second the internal motions of the adenine residues containing the tract  $\text{A}_3\text{T}_3$  with those of the other residues, we present here an NMR investigation of the C1'H1' and of the C5'H5' or C5'H5'' dynamic processes of the dodecamer  $\text{d}(\text{CGCAAATTTGCG})_2$  selectively  $^{13}\text{C}$  and  $^{13}\text{C}$  labeled on the C3, A4 and A6 residues.

## EXPERIMENTAL

$[1',5'\text{-}^{13}\text{C}]\text{-dA}$  and  $[1',5'\text{-}^{13}\text{C}]\text{-dC}$  were prepared by *N*-glycosylation as reported.<sup>7</sup> The required  $1',5'\text{-}^{13}\text{C}$ -

\* Correspondence to: G. Lancelot.

labeled oligodeoxynucleotide was prepared on a Pharmacia automatic synthesizer via phosphoramidite chemistry using the classical unlabeled or  $[1',5'\text{-}^{13}\text{C}]$ -labeled deoxynucleotide 5'-O-dimethoxytrityl-3'-O-( $\beta$ -cyanoethyl-*N,N*-diisopropylphosphoramidite) building block.<sup>8</sup> After deprotection, the oligodeoxynucleotide was purified by anion-exchange chromatography on a mono-Q column (Pharmacia) and analyzed by reversed-phase HPLC.

### NMR samples

Oligonucleotide solutions were passed through a Chelex-100 column to remove paramagnetic impurities and adjusted to pH 7.0, then lyophilized from  $\text{D}_2\text{O}$  and dissolved in  $\text{D}_2\text{O}$  containing 0.1 M NaCl. The NMR samples (1.5 mm) were degassed and were kept in sealed tubes.

### NMR spectroscopy and relaxation rate measurements

NMR experiments were performed between 17 and 47 °C on a Bruker AMX-500 spectrometer and processed on an X32 computer.  $^1\text{H}$  and  $^{13}\text{C}$  NMR spectra were recorded at 500.139 and 125.770 MHz, respectively. The  $^1\text{H}$  and  $^{13}\text{C}$  90° pulses were 10.0 and 27.2  $\mu\text{s}$ , respectively, at 22 °C and were adjusted for each temperature. An increase of 27% in their values was observed between 17 and 47 °C.

The NOESY spectra were recorded with 1024 complex data points and a spectral width of 5500 Hz. The evolution delay in the  $t_1$  dimension was incremented in 512 equal steps of 100  $\mu\text{s}$ , resulting of a 5120 Hz width. Eight NOESY spectra were obtained at 32 °C at mixing times of 0, 30, 50, 75, 100, 150, 200 and 300 ms. The preparation delay was 2 s, which allows at least 80% magnetization recovery of all the protons. Cross peak volumes were measured using the UXNMR software. The intranucleotide H5–H6 NOE of the C3 and C11 residues (overlapped resonances) was computed as the ratio of the corresponding cross peak volume with the volume of the diagonal peak measured on the same row at a zero mixing time. The  $^1\text{H}$  chemical shifts are given relative to 4,4-dimethyl-4-silapentane-1-sulfonate (DSS) as an internal reference.

The relaxation rates  $R(\text{C}_z)$ ,  $R(\text{C}_{x,y})$  and  $R(\text{H}_z \rightarrow \text{C}_z)$  were measured following the pulse sequences described previously.<sup>1,9</sup> Heteronuclear spin-lock and proton irradiation during the relaxation period were used in order to decouple the cross-relaxation pathways during the relaxation experiments, and to approach mono-exponential behavior as closely as possible.<sup>10,11</sup>  $T_1$  and  $T_{1\rho}$  curves were fitted with 12 data points at 0, 50, 100, 150, 200, 250, 300, 350, 400, 450, 500 and 600 ms and 0, 20, 40, 60, 80, 100, 130, 180, 220, 250, 300 and 400 ms, respectively. In the  $T_{1\rho}$  experiment, the spin-lock was constituted by contiguous phase-alternating 180°  $^{13}\text{C}$  pulses at low power. These 180° pulses were adjusted at each temperatures. Various r.f. field strengths ( $\nu_{\text{SL}} = 746, 1205, 1923, 2416, 3012, 3732$  and 4808 Hz) were obtained by adjusting the pulse length at different power levels. The spin-lock carrier frequency was set on

the  $^{13}\text{C}1'$  resonance of the A4 residue, leading to an offset of 186 and 23 Hz for the  $^{13}\text{C}1'$  resonances of the C3 and A6 residues, respectively. The accuracy of  $R(\text{C}_{x,y})$  was improved by correcting the effective spin-lock field using Eqn (9) in the paper by Peng *et al.*<sup>12</sup> The  $^{13}\text{C}5'$  values were measured with the spin-lock carrier frequency set on the middle of the overlapped  $^{13}\text{C}5'$  resonances and no correction was applied. In order to estimate accurately the heteronuclear NOE value,  $R(\text{H}_z \rightarrow \text{C}_z)$  was measured for cross relaxation delays of 1, 1.2, 1.5 and 2 s and a delay between scans of 4 s. No proton  $T_1$  correction was made to the NOE values. Within the experimental errors, no difference were observed in NOE measured by using the different cross relaxation delays. Areas were calculated with the integration routines of the UXNMR software package. Two series of  $T_1$  and  $T_{1\rho}$  measurements and four series of NOE measurements were performed at each temperature.

Curve fitting was performed using a least-squares program<sup>13</sup> to minimize the value of  $\chi^2$ . Uncertainties were obtained from the covariance matrix as already described<sup>2</sup> and given at a 90% confidence interval. The  $R(\text{C}_z)$ ,  $R(\text{C}_{x,y})$  and  $R(\text{H}_z \rightarrow \text{C}_z)$  values are given with a relative precision of 3, 6, and 8%, respectively. All the deviations of the data between the series of  $T_1$ ,  $T_{1\rho}$  and NOE experiments with the same relaxation delay or cross relaxation delays were running within the corresponding indicated precision.

## RESULTS

### Assignment of the $^1\text{H}1'$ resonances

Figure 1 shows an expansion of the H8/H6–H1' NOESY connectivities of the dodecamer  $\text{d}(\text{CGAAATTTGCG})_2$  at 22 °C. All the aromatic and H1' resonances were easily assigned by using the proximities of the aromatic protons H6/H8 with the H1' protons belonging to their own residue or to their 5'-neighboring residues. The connectivities involving the other sugars and the  $\text{H5}(n)/\text{CH3}(n)\text{--H6}(n-1)/\text{H8}(n-1)$  cross peaks are in agreement with this assignment.

### $^{13}\text{C}\text{--}1'$ spin-lattice relaxation rate measurements

The spin-lattice relaxation rates of the C3, A4 and A6 residues were measured at different temperatures between 17 and 47 °C. Table 1 shows that below 29 °C, the  $R(\text{C}_{x,y})$  value of the C3 residue was always weaker than the adenine residues values by a difference of  $2.7 \pm 0.1 \text{ s}^{-1}$  and that above 29 °C, the  $R(\text{C}_{x,y})$  value of the A4 residue was always higher than the other values of C3 and A6. Moreover, the  $R(\text{H}_z \rightarrow \text{C}_z)$  value was always different between the three labeled residues. These data provide evidence for a different dynamic behavior for the three residues. Table 1 gives the best fit obtained by analyzing these data with the two-parameter Lipari and Szabo approach.<sup>14,15</sup> For all the temperatures, except 47 °C, the order parameter  $S^2$  is

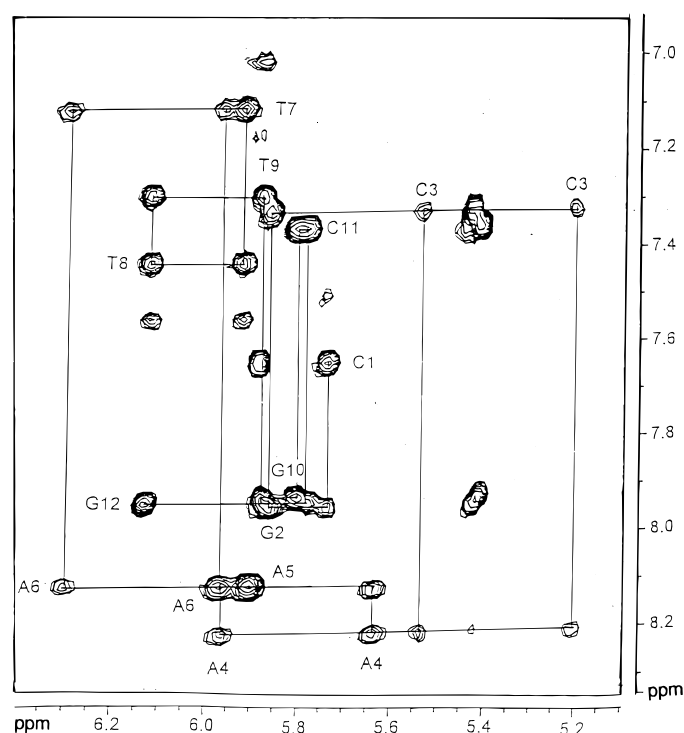


**Figure 1.** Expansion of the NOESY spectra of the  $^{13}\text{C}$ -labeled duplex  $\text{d}(\text{CGCAAATTTGCG})_2$  in  $\text{D}_2\text{O}$ , 1.5 mM at  $22^\circ\text{C}$ , 0.1 M NaCl. The mixing time was 200 ms. The double connectivities implicating the C3, A4 and A6 resonances indicate the  $^{13}\text{C}$  labeling of these residues.

$0.80 \pm 0.02$  for A4 and A6 and  $0.65\text{--}0.73$  for C3. The effective correlation time is in the range 15–31 ps, but these values were spoiled by too large an uncertainty to make each difference indicative. Nevertheless,  $\tau_e$

increased significantly with increase in temperature for the three residues. It can be pointed out that, reflecting the difference between the  $R(\text{C}_{x,y})$  values, the global correlation time changed significantly from the adenine to the cytosine residues at the same temperature.

**Table 1.** Experimental values of the  $^{13}\text{C}1'$  relaxation rates in  $\text{d}(\text{CGCAAATTTGCG})_2$  at various temperatures with,  $\tau_g$ ,  $S^2$  and  $\tau_e$  computed by using the Lipari–Szabo relationship<sup>14,15</sup>

| $T$ ( $^\circ\text{C}$ ) | Residue | $R(\text{C}_2)$ | $R(\text{C}_{x,y})$ | $R(\text{H}_2 \rightarrow \text{C}_2)$ | $\tau_g$ (ns) | $S^2$ | $\tau_e$ (ps) |
|--------------------------|---------|-----------------|---------------------|--|---------------|-------|---------------|
| 17                       | C3      | 1.75            | 21.9                | 0.14                                   | 5.85          | 0.74  | 26            |
|                          | A4      | 1.69            | 24.5                | 0.11                                   | 6.21          | 0.75  | 18            |
|                          | A6      | 1.79            | 24.5                | 0.10                                   | 5.96          | 0.82  | 15            |
| 22                       | C3      | 2.09            | 18.3                | 0.17                                   | 4.79          | 0.74  | 31            |
|                          | A4      | 1.96            | 21.0                | 0.13                                   | 5.25          | 0.79  | 20            |
|                          | A6      | 2.04            | 20.9                | 0.12                                   | 5.09          | 0.81  | 16            |
| 24.5                     | C3      | 2.18            | 16.6                | 0.18                                   | 4.42          | 0.72  | 30            |
|                          | A4      | 2.14            | 19.5                | 0.14                                   | 4.80          | 0.79  | 23            |
|                          | A6      | 2.26            | 19.3                | 0.13                                   | 4.58          | 0.82  | 19            |
| 27                       | C3      | 2.38            | 15.0                | 0.20                                   | 3.94          | 0.72  | 31            |
|                          | A4      | 2.42            | 18.5                | 0.16                                   | 4.33          | 0.82  | 29            |
|                          | A6      | 2.47            | 18.1                | 0.14                                   | 4.19          | 0.72  | 31            |
| 29.5                     | C3      | 2.39            | 13.9                | 0.23                                   | 3.82          | 0.68  | 37            |
|                          | A4      | 2.44            | 17.5                | 0.18                                   | 4.22          | 0.79  | 35            |
|                          | A6      | 2.64            | 16.8                | 0.19                                   | 3.92          | 0.81  | 39            |
| 32                       | C3      | 2.54            | 13.0                | 0.24                                   | 3.52          | 0.68  | 38            |
|                          | A4      | 2.60            | 16.8                | 0.20                                   | 3.98          | 0.80  | 42            |
|                          | A6      | 2.85            | 15.7                | 0.20                                   | 3.58          | 0.82  | 40            |
| 37                       | C3      | 2.75            | 11.3                | 0.26                                   | 3.04          | 0.66  | 38            |
|                          | A4      | 2.86            | 15.2                | 0.23                                   | 3.54          | 0.79  | 49            |
|                          | A6      | 3.15            | 14.0                | 0.25                                   | 3.15          | 0.80  | 54            |
| 42                       | C3      | 2.92            | 10.4                | 0.28                                   | 2.75          | 0.64  | 39            |
|                          | A4      | 3.12            | 13.7                | 0.27                                   | 3.15          | 0.78  | 59            |
|                          | A6      | 3.36            | 12.3                | 0.32                                   | 2.81          | 0.76  | 69            |
| 47                       | C3      | 2.79            | 10.7                | 0.27                                   | 2.91          | 0.64  | 38            |
|                          | A4      | 2.94            | 13.9                | 0.27                                   | 3.33          | 0.76  | 56            |
|                          | A6      | 3.16            | 11.6                | 0.32                                   | 2.84          | 0.71  | 55            |

Are the three relaxation rates governed by the same relaxation processes? Before drawing a general conclusion from these results, the influence of the asymmetric shape of DNA needs to be tested. The duplex was modeled by a cylinder with a length ( $12 \times 3.4 = 40.8$  Å) twice the diameter (20.5 Å). Then the ratio between the translational  $D_{\parallel}$  and rotational  $D_{\perp}$  diffusion coefficient was taken as 2.2.<sup>16,17</sup> The spectral density  $J(\omega)$  were computed with the equation<sup>18</sup>

$$J(\omega) = S^2/4[(3 \cos^2 \theta - 1)j(\tau_1) + 3 \cos^2 \theta \sin^2 \theta j(\tau_2) + 3/4 \sin^2 \theta j(\tau_3)] + (1 - S^2)j(\tau_i) \quad (1)$$

with  $j(\tau) = 2/5\tau/(1 + \omega^2\tau^2)$ ,  $\tau_1 = 6D_{\parallel}$ ,  $\tau_2 = D_{\parallel} + 5D_{\perp}$  and  $\tau_3 = 4D_{\parallel} + 2D_{\perp}$ .

Using the solution structure of  $\text{d}(\text{CGCAAATTTGCG})_2$ ,<sup>19</sup> we computed a polar angle  $\theta$  value of  $83^\circ$ ,  $76^\circ$  and  $88^\circ$  for the  $\text{C}1'\text{H}1'$  vector of C3, A4 and A6 residues, respectively. These angles, which led to small variations (5%) of the density functions, are not able to explain the difference in the  $R(\text{C}_{x,y})$  values of the different residues.

We concluded that our data were not fitted well with a single value of  $\tau_g$  using the two-parameter model-free formalism. A good fit of the data of the three residues needs a 12–20% variation of the global correlation time, depending of the temperature, whereas it should be invariant along the sequence for the same temperature. Hence these simple equations cannot agree with the whole set of experimental data.

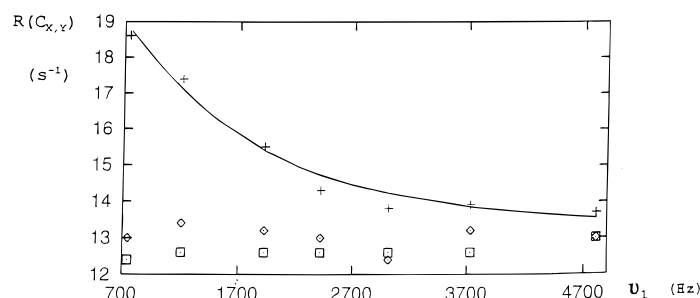


**Figure 2.** Plot of  $R(C_{x,y})$  at 32 °C vs. the spin-lock power  $\nu_1$ . The curve represents the fit of Eqn (3) to the experimental data.  $R_d(C_{x,y}) = 13.0 \text{ s}^{-1}$ ,  $\tau_{\text{ex}} = 130 \text{ }\mu\text{s}$ ,  $\Delta\omega^2 p_1 p_2 = 61\,000 \text{ rad}^2 \text{ Hz}^2$ . ( $\square$ ) C3; (+) A4; ( $\diamond$ ) A6.

**Additional relaxation pathways induced by slow motions.** In order to explain the relaxation rate difference along the sequence of the duplex  $d(\text{CGCAAATTTGCG})_2$ , the relative contribution of each possible relaxation process requires estimation. Taking into account that paramagnetic impurities such as cations or oxygen were carefully removed, relaxation processes involving paramagnetic impurities can be ruled out. Scalar relaxation of the second kind<sup>20</sup> could affect the spin-spin relaxation of the C1' through an indirect one-bond interaction if N1 (in the pyrimidines) or N9 (in the purines) relaxed unusually rapidly. However,  $^{13}\text{C}$  spin-lock during the relaxation delay destroyed any scalar spin coupling effects. Consequently, scalar relaxation of the second kind cannot be taken into consideration under our experimental conditions. Chemical shift anisotropy relaxation, which has already been calculated to contribute only 2% to the total relaxation,<sup>2</sup> cannot markedly increase the  $R(C_{x,y})$  relaxation rate. Consequently, differences in the three relaxation rates, and more particularly in  $R(C_{x,y})$ , for different residues in the same oligonucleotide could be attributed to additional slow motions or to chemical exchange.

**Exchange relaxation.** NMR chemical exchange processes are efficient when the exchange time-scale is in the range of the inverse of the resonance frequency difference between the two exchanging sites. This leads to exchange time-scales in the range of microseconds to seconds. Consequently, only components implicating low frequency are modified and the term  $R_{\text{ex}}$  is efficient on the spin-lattice relaxation rate  $R(C_{x,y})$  only. For a two-step exchange process, the exchange contribution to  $R_{\text{ex}}(C_{x,y})$  is related by the equation<sup>21</sup>

$$R_{\text{ex}} = (\Delta\omega)^2 p_1 p_2 \tau_{\text{ex}} / (1 + \omega_1^2 \tau_{\text{ex}}^2) \quad (2)$$

where  $p_1$  and  $p_2$  are the populations of the two conformers,  $\Delta\omega$  the resonance frequency difference between the exchanging sites and  $\omega_1$  the equivalent frequency of the applied r.f. field. In this case,  $R(C_{x,y})$  is the sum of the dipolar contribution  $R_d(C_{x,y})$  and of the exchange contribution:

$$R(C_{x,y}) = R_d(C_{x,y}) + R_{\text{ex}} \quad (3)$$

The dependence of  $R(C_{x,y})$  on the applied r.f. field strength  $\omega_1 = -\gamma B_1$  for the C3, A4 and A6 residues at 32 °C is shown in Fig. 2. The  $R(C_{x,y})$  values of C3 and A6 were constant within the experimental uncertainty. On the other hand, the  $R(C_{x,y})$  values of A4 decreased with  $\omega_1$  and tended toward a plateau for  $\nu_1 > 3000 \text{ Hz}$ , giving direct evidence of exchange processes for the

$^{13}\text{C}1'$  resonance of A4. The exchange lifetime  $\tau_{\text{ex}}$  was derived by fitting  $R(C_{x,y})$  with a least-squares program<sup>13</sup> computing Eqn (3) (Fig. 2). The best fit was obtained with  $\tau_{\text{ex}} = 130 \text{ }\mu\text{s}$ ,  $(\Delta\omega)^2 p_1 p_2 = 61\,000 \text{ rad}^2 \text{ Hz}^2$  and  $R_d(C_{x,y}) = 13 \text{ s}^{-1}$ .

If we assume that  $p_1$  is in the range 0.1–0.5, the apparent frequency difference between the two exchanging sites of A4 is estimated to be in the range 130–250 Hz. These frequency differences between the different conformational states implicate large amplitude motions such as several tens of a degree or several tenths of an angstrom. They can be favored by the strong ring current effects of the adenines which governed the  $^{13}\text{C}1'$  chemical shift variations of their neighboring bases. Such a dynamic process can be related to a special structure characterized by a gradual and increasingly compressed minor groove which reached a minimum at the ApT step.<sup>22</sup>

**Analysis of the spin-lattice relaxation rate including the exchange.** The spin-lattice relaxation rates of the three residues were fitted after subtraction of  $R_{\text{ex}}$  from  $R(C_{x,y})$  for A4. The best fit was obtained with a unique correlation time of 3.66 ns and an order parameter of 0.73, 0.75 and 0.83 for C3, A4 and A6, respectively, at 32 °C. In order to validate this analysis, an independent measure of  $\tau_{\text{g}}$  using a proton cross relaxation rate was made. The H5–H6 NOE build-up rates of C3 and C11 (overlapped resonances) (Fig. 1) were measured at eight different mixing times. The simulated NOE were made by using the RELAZ program,<sup>23</sup> which computes the NOE after diagonalization of the complete relaxation matrix.<sup>24</sup> The best fit (Fig. 3) was obtained with a global correlation time of  $3.4 \pm 0.4 \text{ ns}$  by using the conformation and the surrounding of the C3 residue computed in

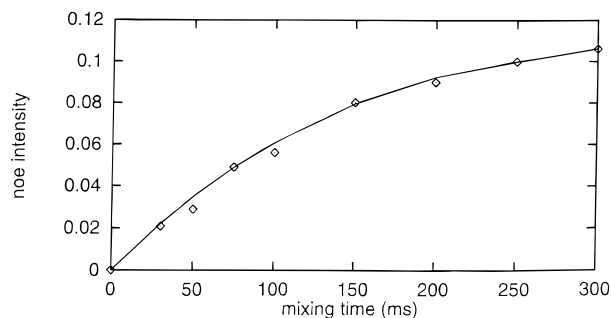


**Figure 3.** Plot of the NOE between H5 and H6 for C3 and C11 (average of the two values) measured at 32 °C vs. the mixing time. The curve represents the computed NOE (see text) with a global correlation time of 3.4 ns.

**Table 2.** Experimental values of the  $^{13}\text{C}'$  relaxation rates in  $\text{d}(\text{GCGAAATTTGCG})_2$  at various temperatures, with  $\tau_g$ ,  $S^2$  and  $\tau_s$  computed by using the Lipari–Szabo relationship<sup>14,15</sup>

| $T$ ( $^{\circ}\text{C}$ ) | $R(\text{C}_z)$ | $R(\text{C}_{x,y})$ | $R(\text{H}_z \rightarrow \text{C}_z)$ | $\tau_g$ (ns) | $S^2$ | $\tau_s$ (ns) |
|----------------------------|-----------------|---------------------|--|---------------|-------|---------------|
| 22                         | 1.85            | 7.40                | 0.25                                   | 3.15          | 0.41  | 26            |
| 27                         | 2.19            | 6.21                | 0.31                                   | 2.46          | 0.41  | 32            |
| 32                         | 2.38            | 5.67                | 0.29                                   | 2.05          | 0.42  | 27            |
| 37                         | 2.57            | 4.83                | 0.43                                   | 1.71          | 0.37  | 44            |

the solution structure.<sup>19</sup> This value is in agreement with  $\tau_g = 3.66$  ns computed via the  $^{13}\text{C}$  relaxation rates and with the already published  $^{13}\text{C}$  relaxation rate measurements on the three central thymines of the same oligonucleotide which gave  $\tau_g = 3.3$  ns at  $32^{\circ}\text{C}$ .

### $^{13}\text{C}$ -5' spin–lattice relaxation rate measurements

The  $\text{H}5'$ – $\text{H}5''$  resonances and the  $^1\text{H}$ – $^{13}\text{C}'$  correlations appeared too overlapped to allow separate relaxation rate measurements for each residue. Consequently, Table 2 gives the average of the  $R(\text{C}_z)$ ,  $R(\text{C}_{x,y})$  and  $R(\text{H}_z \rightarrow \text{C}_z)$  values for C3, A4 and A6. Taking into account that the carbon  $\text{C}5'$  is bound to two hydrogen atoms,  $R(\text{C}_z)$  and  $R(\text{C}_{x,y})$  were computed by dividing the inverse of  $T_1$  and  $T_{1\rho}$  by two. The analysis of these data with the two parameter Lipari and Szabo relationship showed order parameters weaker than those of the  $^{13}\text{C}1'$  resonances for the same temperature. Nevertheless, the global correlation time computed at  $32^{\circ}\text{C}$  (2 ns) is different than those computed for the  $\text{C}1'$  resonance (3.7 ns), indicating supplementary pathways of relaxation. Introduction of an additional slow motion<sup>25</sup> led to  $S_f^2 = 0.50$ ,  $S_s^2 = 0.61$ ,  $\tau_s = 1$  ns,  $\tau_f = 2.5$  ps with

$\tau_g$  fixed at 3.7 ns. It can be pointed out that this analysis was made by assuming that the relaxation rates of the three residues are close. This assumption may not be valid, in which case the curves will not be exponential and the fit error will be substantially higher. Consequently, attempts to relate these data with more accurate analysis seems hazardous at this time.

### CONCLUSION

The three relaxation rates  $R(\text{C}_z)$ ,  $R(\text{C}_{x,y})$  and  $R(\text{H}_z \rightarrow \text{C}_z)$  were accurately measured for three residues in the duplex  $\text{d}(\text{GCGAAATTTGCG})_2$ . For each temperature, the three residues exhibited fast motions on the time-scale of a few picoseconds. This fast process could correspond to the motion of the sugar around the glycosidic bond.<sup>2</sup> The r.f. field strength dependence of the  $R(\text{C}_{x,y})$  values of  $\text{C}1'$  provided evidence for an exchange process for the A4 residue at  $32^{\circ}\text{C}$ . It can be pointed out that no additional relaxation pathways induced by slow motions have been observed for the other labeled residues (C3, A6, T7, T8 and T9).<sup>2</sup> The exchange process of the adenine residue is favored by the important ring current of this base. This additional relaxation process was analyzed in terms of chemical exchange between distinct conformational states involving large amplitude and slow (130  $\mu\text{s}$ ) motions which can reflect special dynamics of the tract  $\text{A}_3\text{T}_3$  which supports the spine of hydration.<sup>26</sup> The relaxation rates of the  $\text{C}5'$  carbon provided evidence for internal motions with higher amplitude than for  $\text{C}1'$ . These weak order parameters are in agreement with the additional motions undergone by the  $\text{C}5'\text{H}5'$  or  $\text{C}5'\text{H}5''$  vectors, such as repuckering of sugars and rotation around the  $\text{C}4'$ – $\text{C}5'$  bond.

### REFERENCES

- J. W. Peng and G. Wagner, *J. Magn. Reson.* **98**, 308 (1992).
- F. Gaudin, F. Paquet, L. Chanteloup, J. M. Beau, N. T. Thuong and G. Lancelot, *J. Biomol. NMR* **5**, 49 (1995).
- D. M. Crothers, T. E. Haran and J. G. Nadeau, *J. Biol. Chem.* **265**, 7093 (1990).
- P. J. Hagerman, *Nature (London)* **321**, 449 (1986).
- J. L. Leroy, E. Charretier, E. Kochoyan and M. Guéron, *Biochemistry* **27**, 8894 (1988).
- D. G. Brown, M. S. Sanderson, E. Garman and S. Neidle, *J. Mol. Biol.* **226**, 481 (1992).
- L. Chanteloup and J. M. Beau, *Tetrahedron Lett.* **33**, 5347 (1992).
- H. Vorbrüggen, K. Krolkiewicz and B. Bennua, *Chem. Ber.* **114**, 1234 (1981).
- L. E. Kay, L. K. Nicholson, F. Delaglio, A. Bax and D. A. Torchia, *J. Magn. Reson.* **97**, 359 (1992).
- J. Boyd, U. Hommel and I. D. Campbell, *Chem. Phys. Lett.* **175**, 477 (1990).
- A. G. Palmer, M. Rance and P. E. Wright, *J. Am. Chem. Soc.* **113**, 4372 (1991).
- J. W. Peng, V. Thanabal and G. Wagner, *J. Magn. Reson.* **94**, 82 (1991).
- G. Lancelot, *Biochimie* **59**, 587 (1977).
- G. Lipari and A. Szabo, *J. Am. Chem. Soc.* **104**, 4546 (1982).
- G. Lipari and A. Szabo, *J. Am. Chem. Soc.* **104**, 4559 (1982).
- M. M. Tirado and J. Garcia de la Torre, *J. Chem. Phys.* **71**, 2581 (1979).
- M. M. Tirado and J. Garcia de la Torre, *J. Chem. Phys.* **73**, 1986 (1980).
- D. E. Woessner, *J. Chem. Phys.* **37**, 647 (1962).
- F. Gaudin, D. Genest and G. Lancelot, to be published.
- A. Abragam, *The Principles of Nuclear Magnetism*. Oxford University Press, Oxford (1961).
- M. J. Blackledge, R. Brüschweiler, C. Griesinger, J. M. Schmidt, P. Xu and R. R. Ernst, *Biochemistry* **32**, 10960 (1993).
- A. A. Lipanov and V. P. Chuprina, *Nucleic Acids Res.* **15**, 5833 (1987).
- G. Lancelot, J. L. Guesnet and F. Vovelle, *Biochemistry* **28**, 4982 (1990).
- J. W. Keepers and T. L. James, *J. Magn. Reson.* **57**, 404 (1984).
- G. M. Clore, P. C. Driscoll, P. T. Wingfield and A. M. Gronenborn, *Biochemistry* **29**, 7387 (1990).
- H. R. Drew and R. E. Dickerson, *J. Mol. Biol.* **151**, 535 (1981).